EXPERIMENTAL STUDIES OF BEAM DYNAMICS NEAR THE LINEAR COUPLING RESONANCE

P.F.Tavares, A.L.Xavier Jr., Liu Lin, L.Jahnel, and R.H.A.Farias
Laboratório Nacional de Luz Síncrotron, Campinas, Brazil

Abstract

We study the dynamics of transverse oscillations near the linear coupling resonance excited by a pair of skew quadrupoles at the LNLS UVX electron storage ring through the analysis of the beam profile. Transverse oscillations were excited with a fast kicker and the resulting oscillating beam profile was observed by focussing visible synchrotron radiation from a bending magnet onto a fast ccd camera. A least-squares fit of the experimentally obtained isointensity contours to the calculated beam profile border provides a new method to determine both the modulus and phase of the coupling coefficient. The values obtained for the modulus are in good agreement with those from tune separation determination methods and the values obtained for the phase agree with calculations based on the model lattice and the known skew quadrupole distribution.

1 INTRODUCTION

Coupling between the horizontal and vertical motion (Betatron coupling) is widely recognized[1] as an important performance limitation in storage rings used as synchrotron radiation sources or as colliders. The LNLS 1.37 GeV UVX electron storage ring has shown the effects of betatron coupling since the early commissioning stages. In fact, at injection energy (120 MeV), the observed coupling is much larger than expected from simulations, which led us to start an experimental program to determine the origins of coupling in our machine.

In this work, we present an experimental study of the linear coupled transverse beam dynamics in the vicinity of the $\nu_x - \nu_y = 3$ resonance excited by skew quadrupoles. We introduce a new experimental technique to obtain the parameters characterizing the strength of the resonance (namely the modulus and phase of the coupling coefficient). The method consists in observing the time evolution of the transverse beam profile for a few milliseconds (a short time if compared to the synchrotron damping time, but long compared to the betatron oscillation period) after exciting the beam with a fast (few hundred ns) horizontal kick. The acquired image is a projection onto the xy plane of the phase space density distribution function integrated over a very large number of turns (but still small enough that the system may be considered Hamiltonian). Many of the geometric characteristics of the phase space orbits reveal themselves in this time averaged profile, allowing the direct observation of several aspects of the phase space geometry close to the resonance and the experimental determination of the parameters describing the resonance strength.

2 OUTLINE OF THE THEORY

The Hamiltonian that describes transverse electron motion close to a linear coupling resonance excited by a distribution of skew quadrupoles is given by

$$H(x,x',y,y',s) = \frac{1}{2}x'^2 + \frac{1}{2}y'^2 + \frac{1}{2}K_q(s)x^2 - \frac{1}{2}K_q(s)y^2 + K(s)xy,$$

where x and y are the transverse electron coordinates, primes denote differentiation with respect to the longitudinal coordinate s, $K_q(s)$ describes the normal focussing quadrupoles and

$$K(s) = \frac{ec}{E}\frac{\partial B_x(s)}{\partial x}$$

is the skew quadrupole strength. The equations of motion from this Hamiltonian can be solved exactly in the isolated resonance approximation[2] and the resulting one-turn map is

$$\begin{cases} \dfrac{x(\varphi)}{x_0} = \cos(\nu\varphi)\cos(\nu_{xx}\varphi) - \dfrac{\Delta}{2\nu}\sin(\nu\varphi)\sin(\nu_{xx}\varphi) \\ \dfrac{y(\varphi)}{x_0} = -\sqrt{\dfrac{\beta_y}{\beta_x}}\dfrac{1}{2\nu}\Big(\mathrm{Im}(\kappa)\cos(\nu_{yy}\varphi) + \mathrm{Re}(\kappa)\sin(\nu_{yy}\varphi)\Big)\sin(\nu\varphi) \end{cases}$$

where

$$\nu = \frac{1}{2}\sqrt{|k|^2 + \Delta^2}\ ,$$

$\Delta = \nu_x - \nu_y - 3 \approx 0$, and

$$\nu_{xx} = \nu_x - \frac{\Delta}{2},$$

$$\nu_{yy} = \nu_y + \frac{\Delta}{2}.$$

The complex coupling coefficient is a function of the machine optics and the distribution of coupling elements along the lattice and is given by

$$\kappa = \frac{1}{2\pi}\int_0^L \sqrt{\beta_x\beta_y}K(s)\exp\left\{i\left[\psi_x - \psi_y - (\nu_x - \nu_x - 3)\frac{2\pi s}{L}\right]\right\}ds$$

The one turn map allows us to calculate the average (time integrated) profile in the transverse plane for a beam under linear coupling following a kick. Figure 1 shows an example of transverse profile given by this calculation where the main characteristics of coupling can be directly identified. The beam profile is rotated with respect to the symmetry plane of the machine and the outermost contour is distorted. These geometric properties (rotation and distortion) can be associated with the real and imaginary parts of the coupling coefficient respectively.

The outermost contour of the kicked beam profile can be calculated by considering the radial coordinate R in the xy plane and imposing the condition

$$\frac{dR}{d\varphi} = 0,$$

with the constraint

$$\tan(\gamma) = \frac{y}{x}$$

(which sets the direction in the xy plane at which we calculate the radial position of the outer contour). This leads to a fourth-order polynomial whose roots can be determined numerically. Once this algorithm is available to calculate the profile contour from given values of the coupling coefficients, it can be applied to a fitting routine that searches for the best values of κ to fit a measured beam profile. This provides experimental estimates of both the real and imaginary parts of the coupling strength.

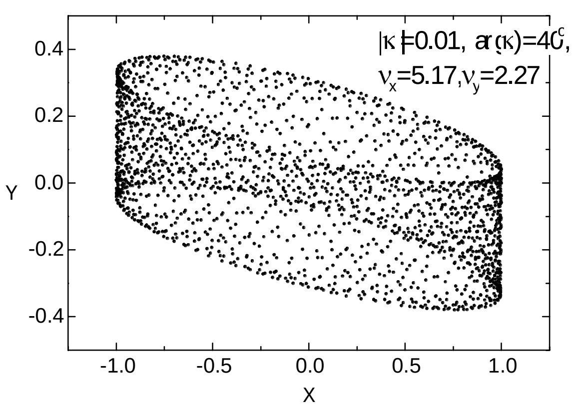

Figure 1: Example of integrated beam transverse profile which results from the calculated transverse map.

3 EXPERIMENTAL RESULTS

The LNLS UVX storage ring

The LNLS UVX electron storage ring is a 1.37 GeV machine injected from a 120 MeV LINAC. The lattice is a six-fold symmetric double-bend achromat with alternating long (non-dispersive) and short (dispersive) straight sections and a total length of 93.21 m). A pair of skew quadrupoles (AQS05A and AQS05B) is installed in one of the long straight sections and was used to drive the coupling resonance. The two skew quadrupoles are located symmetrically with respect to the center of the straight section. One of the injection kickers was used to excite a coherent betatron oscillation and the subsequent evolution of the transverse beam profile was observed with a synchrotron radiation monitor. The beam energy was 600 MeV in order to have a sufficiently long damping time (90 ms) with respect to the image integration time (8.6 ms). In the results reported here, we have operated the storage ring in the low vertical beta optics (Fig. 4). The low vertical optics was implemented in the straight section containing the pair of skew quadrupoles (breaking the six-fold symmetry of the lattice) in order to provide a large vertical betatron phase advance (while keeping the horizontal phase advance small) from one skew quadrupole to the other and thus allow the phase of the coupling coefficient to be varied by powering each skew quadrupole separately.

The optical beam profile monitor

The optical characterization bench uses visible radiation from a low dispersion (4°) bending magnet port. The CCD sensor is an EEV CAM17-46E camera capable of producing non-standard video signals which provide up to 116 Hz frame rate. This is important in order to guarantee that the total frame integration time is small with respect to the synchrotron damping time at the energies of interest. The CCD spatial resolution is 15 µm and the camera output signal is digitized with a Matrox Pulsar frame grabber board which provides 8 bit amplitude resolution and the possibility of using an external trigger signal to start frame acquisition.

Results and Discussion

Each skew quadrupole was powered independently and Figure 2 and Figure 3 show the variation of |κ| as a function of either quadrupole magnet strength. As expected, the modulus of the coupling coefficient is largely insensitive to the betatron phase advance from one quadrupole to the next. Also the slope of both curves agree with the theoretical estimate (|κ| = 0.13 K) based on the model optics to within 15 %. Figure 4 shows the measured change in the phase of the coupling coefficient as we power skew quadrupole A instead of skew quadrupole B as a function of quadrupole strength. This change in phase reflects the large vertical betatron phase advance between the two skew quadrupoles and can be computed once we know the betatron functions at the center of the straight section by

$$\Delta\psi = 2\left[\arctan\left(\frac{S}{\beta_{0x}}\right) - a\tan\left(\frac{S}{\beta_{0y}}\right)\right] - 2\left[\nu_x - \nu_y - 3\right]\frac{S}{L}$$

where s is the distance from the center of the straight section to either skew quadrupole and β_{0x} and β_{0y} are the betatron functions at the center of the section, which are estimated from measurements at the nearby focusing quadrupoles. The resulting calculated change in the phase of the coupling coefficient is 114 degrees which is about 15% above the experimentally determined values.

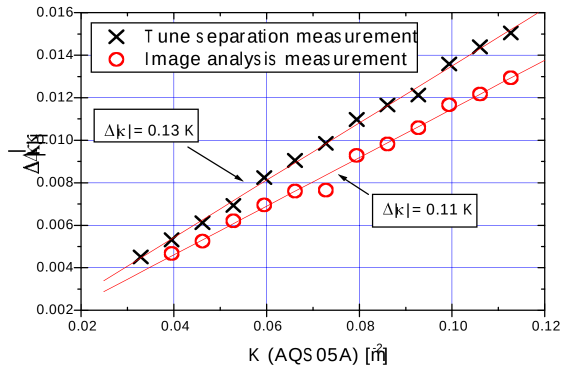

Figure 2: Measurement of the variation of |κ| as a function of quadrupole magnet strength in the low beta optics. Only skew quadrupole A is powered.

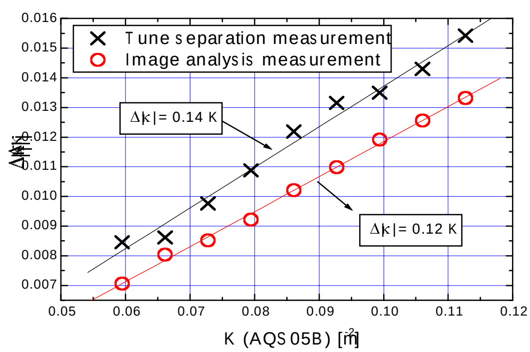

Figure 3: Measurement of the variation of |κ| as a function of quadrupole magnet strength in the low beta optics. Only skew quadrupole B is powered.

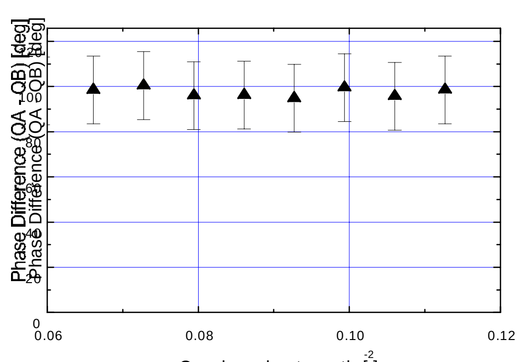

Figure 4: Change in the phase of the coupling coefficient as we power quadrupole A instead of quadrupole B as a function of quadrupole strength in the low beta optics.

Method limitations

We now discuss some limitations of the profile analysis technique for measuring the coupling coefficient and discuss factors that influence the accuracy of the previous results. We estimate the error bars in the coupling coefficient modulus measurements to be ±0.002 in the case of the closest tune approach method. This is given by the tune measurement resolution. In order to estimate the error bars in the coupling measurements via image analysis, we have applied the image analysis algorithm to simulated profiles and calculated the spread in the resulting values of the coupling coefficient as we choose different isointensity contours for the fitting procedure. This gives ± 0.001 for the measurement of the modulus of the coupling coefficient. Those simulations do not take into account the fact that the theoretical analysis given above effectively assumes a single particle beam which means that the beam size must be small with respect to the amplitude of the coherent oscillation. If this is not the case, the beam profile smears out and the determination of the imaginary part of κ (which is more critically dependent on the shape of the profile rather than on its orientation) becomes less precise. Therefore the kicker strength must be chosen so that the oscillation amplitude is large compared to the beam size, yet not so large that non-linearities become important. Also, this implies that the skew quadrupole strength must be small since, on the contrary, large beam sizes will be produced. The error bars in the phase measurements have been determined by simulation to be of the order of 15 degrees for the coupling phases we have measured However, the uncertainty increases considerably for coupling phases close to zero. This happens because, for small coupling phases, large variations in phase cause comparatively little change to the kicked beam profile. Finally the method is limited by the validity of the isolated resonance approximation, i. e., for the tune region where the analytical map correctly represents the motion. This is not really a limitation in the sense that the very significance of the coupling coefficient κ is also restricted to region in tune space where the isolated resonance approach is valid.

ACKNOWLEDGEMENTS

This work has been partly funded by FAPESP under Grants 97/12948-4 and 95/9746-5.

REFERENCES

[1] J. Y. Liu et al, *Determination of the linear coupling resonance strength using two-dimensional invariant tori*, Phys. Rev. E **49**, (1994) 2347.

[2] G. Guignard *A general theory of resonances in accelerators*, CERN Yellow Report 78-11 (1978).